Supercritical Carbon Dioxide: An Inert Solvent for Catalytic Hydrogenation?

Marco Burgener, Davide Ferri, Jan-Dierk Grunwaldt, Tamas Mallat, and Alfons Baiker*

Department of Chemistry and Applied Biosciences, Swiss Federal Institute of Technology, ETH Hönggerberg HCI, CH-8093 Zurich, Switzerland

Received: April 25, 2005; In Final Form: July 1, 2005

Various surface species originating from the reaction between CO_2 and H_2 over Al_2O_3-supported Pt, Pd, Rh, and Ru model catalysts were investigated by attenuated total reflection infrared (ATR-IR) spectroscopy under high-pressure conditions. Two different spectroscopic cells were used: a variable-volume view cell equipped with ATR-crystal and transmission IR windows (batch reactor) and a continuous-flow cell also equipped with a reflection element for ATR-IR spectroscopy. The study corroborated that CO formation from dense CO_2 in the presence of hydrogen occurs over all Pt-group metals commonly used in heterogeneous catalytic hydrogenations in supercritical CO_2 ($scCO_2$). In the batch reactor cell, formation of CO was detected on all metals at 50 and 90 °C, with the highest rate on Pt. Additional surface species were observed on Pt/Al_2O_3 at 150 bar under static conditions. It seems that further reaction of CO with hydrogen is facilitated by the higher surface concentration at higher pressure. In the continuous-flow cell, CO coverage on Pt/Al_2O_3 was less prominent than that in the batch reactor cell. A transient experiment in the continuous-flow cell additionally revealed CO formation on Pt/Al_2O_3 at 120 bar after switching the feed from a H_2−ethane to a H_2−CO_2 mixture. The in situ ATR-IR measurements indicate that CO formation in CO_2−H_2 mixtures is normally a minor side reaction during hydrogenation reactions on Pt-group metal catalysts, and dense ("supercritical") CO_2 may be considered as a relatively "inert" solvent in many practical applications. However, blocking of specific sites on the metal surface by CO and consecutive products can affect structure sensitive hydrogenation reactions and may be at the origin of unexpected shifts in the product distribution.

Introduction

Supercritical carbon dioxide ($scCO_2$) has attracted considerable interest as an alternative reaction medium due to its nonflammability, relative inertness, and low cost—features that are important for industrial applications.[1] There are several reports in heterogeneous and homogeneous catalysis[2,3] on enhanced reaction rate in $scCO_2$ that is mainly attributed to elimination of gas−liquid mass transport limitations. However, in hydrogenation reactions some cases of serious catalyst deactivation were observed, for example during enantioselective hydrogenation reactions.[4,5] It has been proposed that CO is formed as a product of the reverse water−gas shift reaction even

$$H_2 + CO_2 \rightarrow CO + H_2O$$

at low temperature, resulting in poisoning of the noble metal catalyst.[4−7] This assumption is supported by the observation that the change from supercritical carbon dioxide to ethane (scC_2H_6) led to a much higher catalytic activity in the enantioselective hydrogenation of ethyl pyruvate in a continuous-flow fixed-bed reactor.[5] Other routes such as decomposition of reactants and products can also diminish the rate of the target reaction. Arunajatesan et al.[6] reported that peroxides caused severe deactivation in the hydrogenation of cyclohexene over Pd/C in $scCO_2$, which was circumvented using an alumina trap. Very recently, Ichikawa et al.[8] reported a change of selectivity in halonitroaromatics hydrogenation induced by carbon monoxide formation, particularly in $scCO_2$.

Hence, the spectroscopic identification of CO and other possible surface species is required to understand the possible impact on selectivity and activity in hydrogenation reactions. IR spectroscopy is a suitable technique, and a number of studies exist at ambient pressure, where the formation of CO and other reaction intermediates over Rh- and Pd-based catalysts, Ru/TiO_2, and Pt/SiO_2 was investigated.[9−17] Formation of CO from carbonate species on interfacial $Pt−Al_2O_3$ sites of a model catalyst was observed using attenuated total reflection infrared (ATR-IR) spectroscopy in the presence of cyclohexane saturated with 25 vol % CO_2 in hydrogen.[18]

ATR-IR studies in supercritical fluids are rare.[7,19−21] Recently, the gas and liquid-phase water−gas shift and methanol reforming reactions were studied over a pressure range of 1.36−5.84 bar on a 2.1 wt % Pt/Al_2O_3 catalyst deposited on a ZnSe crystal, with CO being either the reactant or the most abundant intermediate.[22] To our knowledge, ATR-IR studies on the reverse water−gas shift reaction over noble metals at elevated pressure have not been reported, despite the fact that noble metals such as Ru, Rh, and Pd are known to catalyze the formation of methane or methanol from CO_2 with adsorbed CO as the intermediate.[10,16,23,24]

The study on the behavior of CO_2 as the solvent at elevated pressure is essential also to gain the spectroscopic evidence that would enable us to answer the question whether $scCO_2$ is an inert solvent for platinum group metal-catalyzed hydrogenation reactions.

We investigated the reverse water−gas shift reaction in $scCO_2$ at different pressures using in situ ATR-IR spectroscopy. For this purpose, thin films of Pt, Pd, Rh, and Ru on Al_2O_3 were

* To whom correspondence should be addressed. Fax: +41 1 632 11 63. E-mail: baiker@chem.ethz.ch.

10.1021/jp0521353 CCC: $30.25
Published on Web 08/12/2005

prepared by physical vapor deposition on ZnSe internal reflection elements (IRE) and were used as model catalysts.[18,25]

Experimental Section

Materials. CO_2 (99.995 vol %), ethane (99.5 vol %), and hydrogen (99.999 vol %) were supplied by CarbaGas. Pt, Pd, Rh (Umicore, 99.9%), Ru (Johnson Matthey, 99.9%), and Al_2O_3 (Balzers, 99.3%) were used for physical vapor deposition.

Film Preparation and Characterization. The thin model films were prepared by electron beam evaporation onto the ZnSe crystal using a Balzers BAE-370 vacuum system.[25] The material (Pt, Rh, Ru, Pd wire, Al_2O_3 tablet) was evaporated from a graphite crucible at a base pressure of about 1×10^{-5} mbar and a deposition rate of 0.5 and 1.0 Å/s for metals and Al_2O_3, respectively. Typically, 100 nm of Al_2O_3 was deposited followed by 1 nm of Pt, Rh, or Ru and 2 nm of Pd. The mass thickness of the films was measured with a sputtering quartz crystal sensor. After each use, the IRE was polished with 0.25 μm diamond paste and thoroughly cleaned with ethanol.

The composition of the thin films was determined by X-ray photoelectron spectroscopy (XPS) performed on a Leybold Heraeus LHS11 apparatus.[26] X-rays were generated by a Mg source (1253.6 eV) operating at 240 W. The spectrometer energy scale was calibrated using the Au $4f_{7/2}$ and Cu $2p_{3/2}$ lines at 84.2 and 932.4 eV, respectively. Spectra were recorded at constant pass energy of 151.0 and 31.5 eV. No charging was observed for the investigated samples.

ATR-IR Spectroscopy. In situ ATR-IR spectra were collected using a Bruker Optics IFS 66/s spectrometer purged with dry air and equipped with a liquid nitrogen-cooled MCT detector. Spectra were acquired by co-adding 200 scans at 4 cm^{-1} resolution.

Experiments under static conditions were performed in a variable-volume high-pressure view cell equipped with an internal reflection element (IRE, ZnSe, trapezoidal, 60°, 27 mm $\times$ 10 mm $\times$ 2 mm, Komlas) in the bottom part and transmission IR windows in the middle part. Detailed description of the cell can be found elsewhere.[20] Experiments that mimic the conditions of the batch reactor were performed at 50 and 90 °C. Typically, after the coated crystal was mounted into the spectroscopic view cell, H_2 at 15 bar was introduced into the cell to reduce the metal surface. After evacuation, a mixture of CO_2 and H_2 was admitted at a pressure increasing from 90 to 130 bar, and spectra were collected.

CO adsorption from the gas phase on the metals was performed for comparison with experiments under elevated pressure. After reduction of the metal with hydrogen, ca. 3 bar CO was admitted into the cell and equilibrated for ca. 30 min with the supported metal film before an ATR-IR spectrum was collected.

A homemade stainless steel cell was used for continuous-flow operation at pressures up to 200 bar. The design of this flow-through high-pressure ATR-IR cell is similar to that previously developed for studying catalytic solid−liquid reactions at ambient pressure.[25,27,28] The IRE (ZnSe, trapezoidal, 45°, 52 mm $\times$ 20 mm $\times$ 2 mm, Komlas) is fixed between two stainless steel plates. A small volume (ca. 0.05 mL) is produced on the IRE using a Viton O-ring, where solutions can flow. Due to the small distance between the plate and the IRE (ca. $^1/_4$ mm) a pressure up to 200 bar can be applied. The ATR cell is mounted on a mirror setting (Optispec) that allows collimation of the IR beam at the entrance and the exit of the IRE to minimize contributions from the O-rings. The in situ cell is equipped with jackets for heat exchange allowing to maintain the temperature at the desired value. The dosing system for compressed gases and liquids as well as pressure release behind the spectroscopic cell corresponds to that previously applied for high-pressure X-ray absorption spectroscopy measurements.[29]

Feeding of compressed carbon dioxide or ethane, hydrogen, and optionally a liquid is done with commercial devices. A CO_2-compressing unit (NWA PM-101) is used for liquid carbon dioxide and ethane. For this purpose, carbon dioxide and ethane are compressed to 150−250 bar and introduced to the in situ cell via a reduction valve with a defined pressure. Hydrogen (at about 180 bar pressure) is added to the system by a six-port valve (Rheodyne 7000), and a liquid can be dispensed with an HPLC pump (Jasco, PU-980). The reaction mixture is admitted to the cell and expanded from 150 bar to normal pressure in an expansion unit (NWA PE-103) where the flow is measured and adjusted. The pressure is measured before the inlet of the reactor cell where also a burst plate is located in order to prevent the cell from unexpected exceeding pressure.

The Pt/Al_2O_3 film was contacted with the CO_2/H_2 mixture (120 bar, 50 °C) in the continuous-flow reactor cell. Typically the average residence time was 0.3 s. In separate experiments, a scC_2H_6/H_2 mixture was allowed to flow before changing to $scCO_2/H_2$. Before admission of any mixture, the metal surface was reduced by H_2 at the same temperature.

Safety Note. The experiments described in this article involve the use of relatively high pressure and require equipment with the appropriate pressure rating.

Results and Discussion

Thin Film Preparation and Characterization. The model catalysts were prepared in the same way as previously reported for the study of liquid−solid reactions at ambient pressure.[25] XPS revealed that all metals were in the reduced state and that alumina homogeneously covered the ZnSe IRE. Signal broadening of the corresponding metal core levels toward high binding energy indicated the presence of a small fraction of oxidized metal.

The detailed characterization of the Pt/Al_2O_3 and Pd/Al_2O_3 model catalysts using scanning tunneling microscopy (STM) and XPS has been reported previously.[25] It has been shown that the film consists of densely packed islands made up of round-shaped metal particles of about 5 nm as determined by STM.[25,30] Pt and Pd on Al_2O_3 exhibited the typical doublet of the Pt 4f and Pd 3d core levels at 71.3 and 74.5 eV and at 340.4 and 355.2 eV, respectively. These values correspond well to those of bulk Pt and Pd.[31,32]

The Ru $3d_{5/2}$ peak was observed at 280.4 eV, which is close to the value for metallic Ru.[33,34] The Rh $3d_{5/2}$ and $3d_{3/2}$ peaks were found at 307.5 and 312.25 eV in good agreement with the reported values for Rh.[35] The metal-to-Al ratio was ca. 1:1 indicating that the alumina layer is partially exposed to the reactants, and the noble metals were present as small islands on top of the Al_2O_3 film. Carbonaceous species corresponding to approximately 20 wt % were also found and are due to exposure of the films to air prior to the XPS and IR measurements and some carbonaceous species from the load lock. Carbon from the air may be present in the form of carbonates and CO adsorbed on the metal surface.

The metallic state of the evaporated thin films was confirmed by CO adsorption from the gas phase. The ATR-IR spectra of adsorbed CO on Pt, Pd, Rh, and Ru were collected after contacting ca. 5 bar (gaseous) CO with the metals at 50 °C in the absence of $scCO_2$ and are depicted in Figure 1. Except for

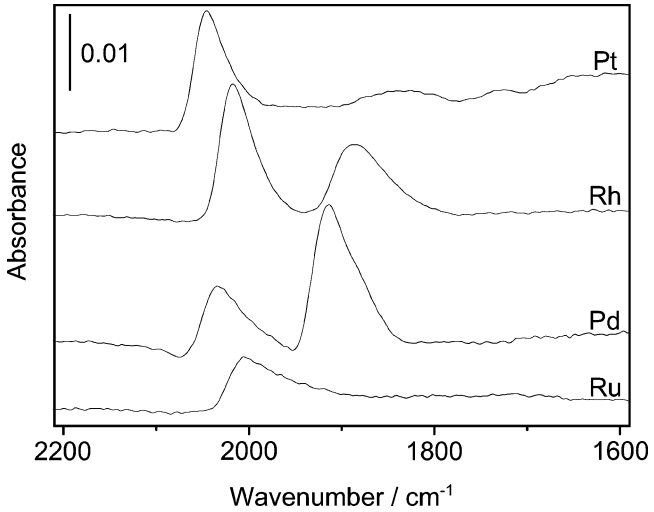

Figure 1. In situ ATR-IR spectra of the Al_2O_3-supported metal films in contact with CO in the variable-volume reactor cell (standard procedure). Conditions: 5 bar CO at 50 °C.

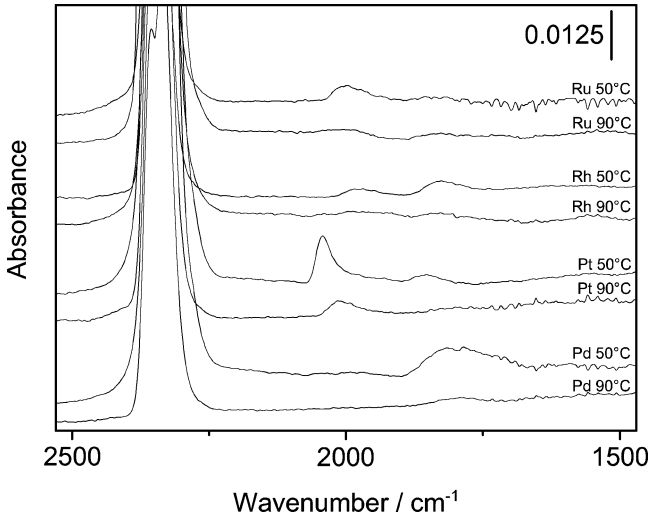

Figure 2. In situ ATR-IR spectra of the Al_2O_3-supported metal films in contact with H_2 and CO_2 in the variable-volume reactor cell at 50 and 90 °C. Conditions: 1 mol % H_2 in CO_2; 100 bar.

Ru, all other metals displayed the typical CO signals corresponding to linear (CO_L) and bridged (CO_B) bonded CO. Bands are observed at 2045 and 1840 cm^{-1} for Pt and at 2018 and 1886 cm^{-1} for Rh. CO on Pd presented the typical larger extinction coefficient for the bridged species than that for the linear species.[36] The low frequency observed for CO on Ru (2006 cm^{-1}) and the absence of additional bands at higher and lower frequencies characteristic of ruthenium carbonyls suggest that the band can be attributed to CO_L on metallic Ru at low surface coverage.[37] The lower affinity of Ru for CO adsorption may indicate that this metal film is also less reactive than the others.

CO Formation from CO_2 in the Presence of H_2 at 100 bar. Figure 2 shows the in situ ATR-IR spectra obtained when contacting the prereduced Al_2O_3-supported metal films with H_2 and CO_2 at 50 and 90 °C in the view cell equipped with a coated IRE.[20] The pressure and temperature range applied here are typical for hydrogenation reactions in $scCO_2$. Under supercritical conditions and in the presence of H_2, the development of signals in the region of adsorbed CO on the different metals is obvious, especially for the Pt/Al_2O_3 film. CO_L was found on Ru (1998 cm^{-1}), Rh (1977 cm^{-1}), and Pt (2042 cm^{-1}). Multicoordinated

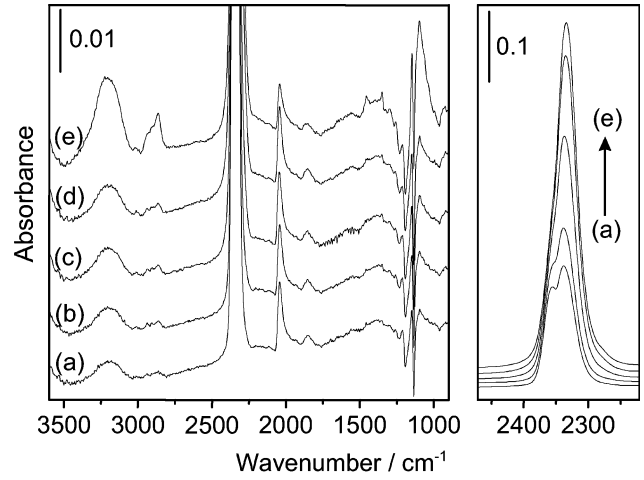

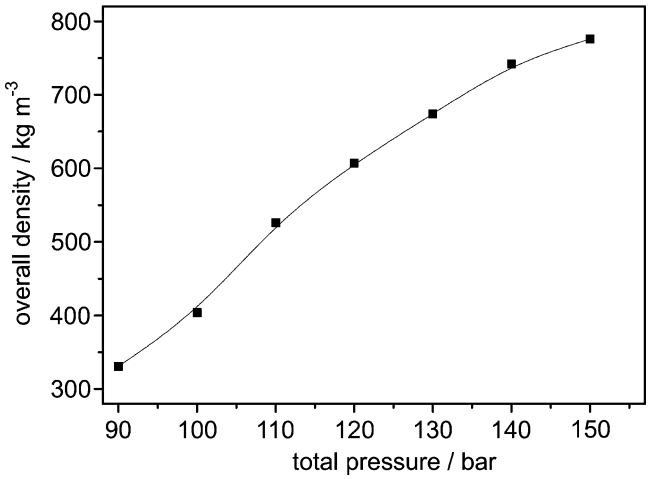

Figure 3. Top panel: pressure-dependent ATR-IR spectra recorded on the Pt/Al_2O_3 thin film in the variable-volume reactor cell. The region of the ν_3 band of CO_2 is shown on the right. Conditions: 1 mol % H_2 in CO_2, 50 °C; (a) 90 bar, (b) 100 bar, (c) 120 bar, (d) 140 bar, (e) 150 bar. For the time dependence see Figure 4. Bottom panel: overall density vs total pressure plot for the same experiment. The density increased with increasing pressure from 331 $kg \cdot m^{-3}$ at 90 bar to 776 $kg \cdot m^{-3}$ at 150 bar.

CO_B was observed on Ru (1827 cm^{-1}), Rh (1828 cm^{-1}), Pt (1859 cm^{-1}), and Pd (1785 cm^{-1}).

The values observed for Pd, Rh, and Ru are lower than those characteristic for CO adsorbed from the gas phase, indicating that the CO coverage is relatively low and that CO could be located at particular metal-support interfacial adsorption sites.[18] The highest CO coverage was found on Pt and Pd at 50 °C, whereas considerably less CO was formed on all metals at 90 °C. Although traces of CO are formed when reducing (cleaning) the metal surface with H_2-saturated solvent in a flow-through cell at normal pressure,[25] no change (e.g., formation of CO or removal of carbonates) was observed in the ATR-IR spectra collected during the H_2 cleaning of the metal films in the batch reactor cell. Hence, this in situ high-pressure study shows that adsorbed CO is formed in the dense CO_2-H_2 mixture. This observation also demonstrates that CO formation is a feasible reaction when hydrogenation reactions are carried out in liquid or supercritical carbon dioxide at elevated pressure.

Surface Species on Pt/Al_2O_3 in $scCO_2/H_2$ at High Pressure. Additional signals appeared in the spectra of Pt/Al_2O_3 in the presence of the CO_2/H_2 mixture while increasing the pressure up to 150 bar. Figure 3 shows some selected ATR-IR spectra to illustrate the effect of pressure; the time dependence is

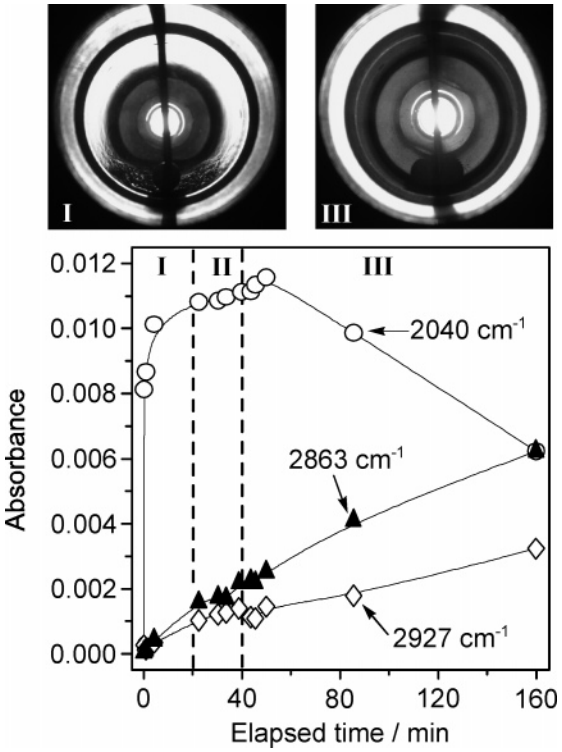

Figure 4. Time-dependent behavior of representative signals of the ATR-IR spectra shown in Figure 3 for Pt/Al_2O_3. Conditions: 1 mol % H_2 in CO_2, 50 °C; (I) 90 bar, (II) 90−140 bar, (III) 150 bar. The lines are drawn to guide the eye. The phase behavior for conditions corresponding to I and III is shown in the top panels.

presented in Figure 4. The signals of adsorbed CO at ca. 2040 and 1859 cm^{-1} increased in intensity with increasing pressure. The difference in density at different pressures also leads to a shift in the asymmetric stretching of CO_2 at 2355 and 2337 cm^{-1} (ν_3 mode). The two characteristic signals coalesced into a stronger singlet at 2334 cm^{-1} when the pressure was increased from 90 to 140 bar, probably due to the loss of the degree of freedom of CO_2 molecules at increasing fluid density (Figure 3, top right panel). Simultaneously, the scissoring mode at 665 cm^{-1} (ν_2, not shown) slowly shifted to 661 cm^{-1}, and the band was also enhanced in the same pressure range indirectly showing the increase of the density.[38] After the ν_3 mode changes into a singlet, its intensity does not substantially increase further above 140 bar, since the density changes only from 742 to 776 $kg \cdot m^{-3}$. Note that in the whole pressure regime one single phase is present in accordance with literature,[39,40] but density fluctuations were observed in the low-pressure regime (Figure 4).

A prolonged study at 150 bar (Figure 4) showed that the CO signals rapidly reached a maximum and were then attenuated with time. Simultaneously to the attenuation of the CO signals at 150 bar, new signals grew at 3212, 2927, 2863, 1457, 1351, and ca. 1100 cm^{-1}. Their size grew with increasing pressure and also with time at 150 bar. The signal at 3212 cm^{-1} is probably due to surface OH groups experiencing surface reorganization because of the occurring reaction and has to be associated with the negative-going band at ca. 3500 cm^{-1}.[25]

The behavior of the signals at 2927, 2863, and ca. 2040 cm^{-1} is shown in Figure 4 as a function of time. The CO coverage rapidly increased when keeping the pressure at 90 bar (I) and was only slightly increased between 90 and 140 bar (II, see also Figure 3). Only traces of the species represented by the other bands could be detected in this pressure range. Between 100 and 140 bar (II) the signals at 2927 and 2863 cm^{-1} did not increase further and were only slightly enhanced at 140−150 bar. CO was clearly consumed when maintaining the pressure at 150 bar, and in parallel the coverage by additional surface species increased (III). The behavior of the bands at 1457, 1351, and 1100 cm^{-1} (not shown in Figure 4 for simplicity) was similar to that of the bands at 2927 and 2863 cm^{-1}. The signals in the C−H stretching region display different kinetic behavior, that is, the growth of the signal at 2927 cm^{-1} exhibited a time delay of about 15−20 min with respect to that at 2863 cm^{-1}. A more detailed analysis of the behavior of the signals as a function of time at 150 bar suggests that the signal at 2927 cm^{-1} is associated with the signals at 1457 and 1100 cm^{-1}, whereas the signal at 2863 cm^{-1} is connected to that at 1351 cm^{-1}. Although the literature available on the reaction between CO and H_2 is copious, the assignment of the signals is not straightforward. The most often observed species during CO_2 hydrogenation are formate-like species.[10,14,41,42] The set of signals at 2863 and 1351 cm^{-1} can be associated with the ν(C−H) and ν_S(OCO) modes of the formate species. However, the ν(C−H) mode of formates is usually found at a higher frequency. A signal at 2920 cm^{-1} was reported on Pt(111),[43] which would suggest that the band at 2927 cm^{-1} originates from formates. This interpretation, however, contradicts the aforementioned combination of the bands and deviates from other values found for formates on Pt single crystals.[44,45]

The set of signals at 2927, 1457, and 1100 cm^{-1} may be assigned to the adsorbed $-OCH_3$ species since the ν(C−H) mode of methyl groups is found at 2960 cm^{-1}. This species is usually unstable and decomposes on Pt(111) to CO already at 150 K under ultrahigh vacuum conditions,[46] but on stepped Pt surfaces its stability is somehow enhanced.[47] The likely explanation is that decomposition of $-OCH_3$ to CO represents the dehydrogenation of methanol via methoxy species and that reaction is effectively catalyzed by all Pt-group metals. The reaction is reversible and in the presence of hydrogen the equilibrium is shifted to the alcohol that is partly present on the surface as alkoxy species. Finally, the signals at 1457, 1351, and 1100 cm^{-1} may also be attributed to formation of carbonates. Despite of this uncertainty, it is very probable that all signals observed in Figure 3 belong to oxygenated C_1 species. The enhancement of the formation of CO and its further transformation to oxygenated C_1 species at 150 bar may be ascribed to the increased surface coverage by hydrogen, which originates from the increase of total pressure that enhances the partial pressure of hydrogen.

CO_2 Hydrogenation in the Continuous-Flow ATR-IR Cell. In addition to the experiments under static conditions, we performed reactions under dynamic conditions in a continuous-flow cell. This reactor has the advantage that different solvents can be used consecutively and the effect of time-on-stream can be studied. Furthermore, mass transfer at the solid−fluid interface is enhanced. Note, however, that the reaction conditions are more difficult to control (biphasic vs monophasic), and the catalyst is more sensitive to impurities in the feed. Besides, in the continuous-flow system much lower conversion is expected, due to the relatively short residence time. The sensitivity of the ATR technique can be enhanced by increasing the number of reflections using a larger crystal (see Experimental Section).

Continuous-flow operation is particularly advantageous to study catalyst deactivation. CO formation was assumed to be responsible for deactivation of a Pd/Al_2O_3 catalyst during citral hydrogenation.[48,49] The proposal was recently reinterpreted in terms of synergic effects of CO formation and hydrocarbon accumulation.[50] CO was also observed as a product of the reverse water−gas shift reaction on a Pd/Al_2O_3 catalyst during

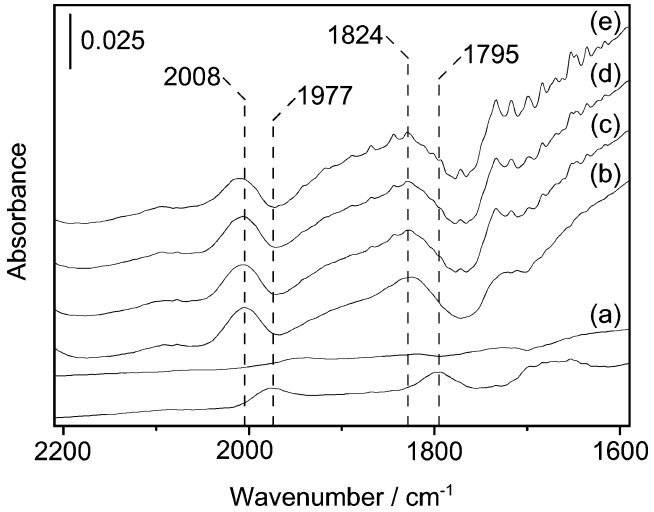

Figure 5. In situ difference ATR-IR spectra (a−e) of a Pt/Al_2O_3 film in contact with 1 mol % H_2 in CO_2 at 120 bar and 50 °C in the continuous-flow reactor cell. The bottom spectrum (without number) is the last spectrum recorded during H_2 cleaning before admittance of $scCO_2/H_2$. Spectrum (e) was recorded after 50 min on stream.

cyclohexene hydrogenation at 70 °C and 138 bar.[51] Furthermore, we have proposed earlier that CO formation could be responsible for the very low reaction rate and enantioselectivity achieved in enantioselective hydrogenations on chirally modified Pt/Al_2O_3 in $scCO_2$.[4,5] The performance of the catalyst improved dramatically when changing from $scCO_2$ to scC_2H_6. To understand this phenomenon, ATR-IR spectra of the Pt surface were recorded during the switch from scC_2H_6/H_2 to $scCO_2/H_2$ mixture in the continuous-flow reactor cell.

Figure 5 shows in situ ATR-IR spectra during the surface-cleaning step in hydrogen and the subsequent admission of the 1% H_2/CO_2 mixture. Already some CO was formed during the surface-cleaning step while the metal film was reduced in situ with H_2 at 5 bar at 50 °C (before admittance of CO_2). Signals at 1977 and 1795 cm^{-1} are due to formation of CO as a result of transformation of impurities present on the metal after exposure of the freshly prepared film to air.[25] Similarly to the case of the solid−liquid interface, the H_2 cleaning affords domains of reduced Pt also at the solid−gas interface. After reduction, CO_2 was admitted to the cell and the total pressure was raised to 120 bar. Then, hydrogen pulses where given in order to produce 1 mol % H_2 in $scCO_2$. The ATR-IR spectra obtained after introducing the first H_2 pulses (lines a−e in Figure 5) displayed features at 2008 and 1824 cm^{-1} together with negative signals at 1977 and ca. 1780 cm^{-1} and the strong ν_3 band of $scCO_2$ (not shown). The positive signals are unambiguously assigned to adsorbed CO on Pt. Interestingly, the vibrational frequency for this species was higher than that detected during H_2 cleaning which, together with the presence of negative signals matching with the signals of CO formed during the reduction of Pt, indicates that additional CO is formed in $scCO_2$ in the presence of H_2.

Next, in a transient experiment the Pt surface was investigated during the change from scC_2H_6/H_2 to $scCO_2/H_2$. Some adsorbed CO was observed in the spectra already in a flow of scC_2H_6 and H_2, most likely due to impurities in the ethane. This observation shows the high sensitivity of the method. Figure 6a presents the spectra in the first 15 min after switching from 1 mol % H_2-in-C_2H_6 to 1 mol % H_2-in-CO_2 mixture.

The characteristic signals of scC_2H_6 at 2974, 2887, 1464, and 1388 cm^{-1} vanish completely, and in parallel the ν_3 band of CO_2 increases with time. Figure 6b shows that upon changing

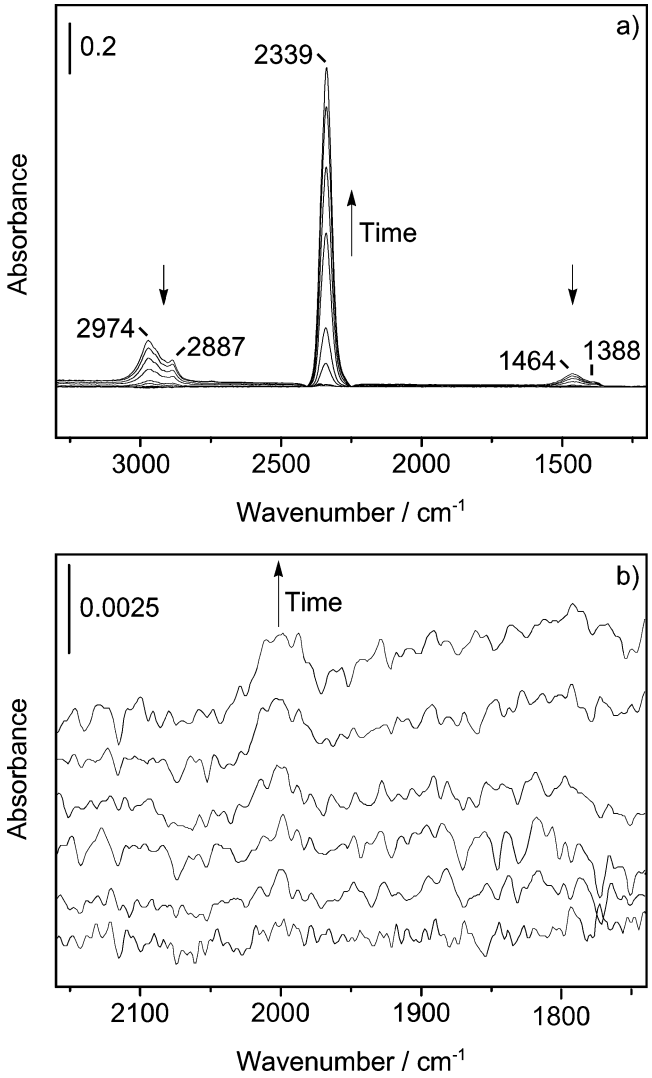

Figure 6. (a) In situ ATR-IR spectra showing the change of the feed composition from 1 mol % H_2-in-C_2H_6 to 1 mol % H_2-in-CO_2 in the continuous-flow reactor cell. Conditions: 50 °C, 120 bar. (b) Difference spectra measured after changing the feed composition. The top spectrum was recorded after 15 min on stream.

the feed composition, a weak signal appeared at ca. 2000 cm^{-1}, which is assigned to adsorbed CO. However, similarly to the case shown in Figure 5, the signal was not as prominent as in the case of the static experiments in the batch reactor cell. This behavior is attributed to the different operation modes and mass transfer conditions in these reactor cells.

Implications to Heterogeneous Catalytic Hydrogenations in Dense CO_2. The results both in the variable volume cell (static conditions) and the continuous-flow cell show that CO can form on Pt-group metals via the reverse water−gas shift reaction when dense CO_2 is used as the solvent in hydrogenation-type reactions, that is, in the presence of hydrogen. Moreover, CO was found to be a possible intermediate in consecutive reactions leading to methanol and formate on Pt. However, the relatively low amount of CO detected in situ in both reactor cells raises the question whether this species can be the origin of catalyst deactivation over noble metal based catalysts. It is expected that in most hydrogenation reactions the low CO coverage on the Pt-group metal surfaces will barely influence the reaction rate. This is in line with the high number of successful hydrogenation reactions reported in heterogeneous catalysis using sub- or supercritical CO_2 as the solvent. We

believe that although dense CO_2 is not truly inert, it remains a valuable solvent for most heterogeneous catalytic hydrogenation reactions.

Nevertheless, in special cases even a small coverage of the metal surface by CO may have a detrimental effect on the catalytic performance. This is the case, for example, when specific surface sites are blocked that are important in the transformation. A known example is the previously mentioned enantioselective hydrogenation over cinchonidine-modified Pt/Al_2O_3.[4−6] In this catalyst system even small amounts of strongly adsorbed CO can disturb the adsorption of the chiral modifier to the metal surface[52,53] and thus its interaction with the prochiral substrate.

From a practical point of view it is more interesting to consider those reactions where even trace amounts of CO have a positive influence on the selectivity. CO formed from CO_2 and H_2 may selectively block specific sites on a polycrystalline metal surface. This effect is expected to be particularly important for low-coordination sites, which are more abundant on nanoparticles typical for supported noble metal catalysts but less plentiful on the extended metal surface of the model catalysts reported in this work. It has been shown that reduction of CO_2 to CO occurs mainly on steps and kinks of Pt single crystal surfaces and CO adsorbs preferentially on steps instead of flat terraces.[54,55]

Selective poisoning of Pt-group metal catalysts by CO is well-known. The industrially most important example is the hydrogenation of acetylene−ethylene mixtures to ethylene in which Pd/Al_2O_3 poisoned by trace amounts of CO is used.[56] After decades of research there is still no agreement concerning the nature of selectivity improvement.[57] Another practically important example is the hydrogenation of 2-chloronitrobenzene over Pt/C.[8] The undesired side reaction, the dechlorination of the main product 2-chloroaniline, was suppressed in $scCO_2$.

Conclusions

The present in situ ATR-IR study shows that CO formation via the reverse water−gas shift reaction from liquid or supercritical CO_2 and hydrogen is a general feature of the commonly used Pt-group metal catalysts (Pt, Pd, Ru, Rh). The CO coverage on all metals under hydrogenation conditions was relatively low so that normally the catalyst performance should not be affected significantly by these adsorbed species. In other words, in many cases $scCO_2$ can be used as a relatively *inert* solvent with all the advantages mentioned in the Introduction. However, the preferential adsorption of CO on step or kink sites as well as its transformation to other adsorbed species may lead to unexpected changes in demanding reactions that occur on specific sites on the catalyst surface. The present study indicates that this selective blocking of active surface sites is crucial for explaining the effect of $scCO_2$ as reaction medium, besides the known factors such as changes in phase behavior, solubility, and mass transfer in the presence of $scCO_2$.

Acknowledgment. The authors gratefully acknowledge the financial support of ETH Zurich and of the "Bundesamt für Energie" (BFE). Moreover, we thank the workshop (R. Mäder, H.-P. Schläpfer, M. Wohlwend) for the support in the high-pressure ATR-IR setups and the construction of the continuous-flow high-pressure ATR-IR cell. M. Caravati is acknowledged for the help during the ATR-IR measurements and B. Benzadi-Arab for preparing of the model films.

References and Notes

(1) Eckert, C. A.; Liotta, C. L.; Bush, D.; Brown, J. S.; Hallett, J. P. *J. Phys. Chem. B* **2004**, *108*, 18108.
(2) Baiker, A. *Chem. Rev.* **1999**, *99*, 453.
(3) Jessop, P. G.; Leitner, W. Introduction − Supercritical Fluids as Media for Chemical Reactions. In *Chemical Synthesis Using Supercritical Fluids*; Jessop, P. G., Leitner, W., Eds.; Wiley-VCH: Weinheim, Germany, 1999; p 1.
(4) Minder, B.; Mallat, T.; Pickel, K. H.; Steiner, K.; Baiker, A. *Catal. Lett.* **1995**, *34*, 1.
(5) Wandeler, R.; Künzle, N.; Schneider, M. S.; Mallat, T.; Baiker, A. *J. Catal.* **2001**, *200*, 377.
(6) Arunajatesan, V.; Subramaniam, B.; Hutchenson, K. W.; Herkes, F. E. *Chem. Eng. Sci.* **2001**, *56*, 1363.
(7) Grunwaldt, J. D.; Wandeler, R.; Baiker, A. *Catal. Rev. − Sci. Eng.* **2003**, *45*, 1.
(8) Ichikawa, S.; Tada, M.; Iwasawa, Y.; Ikariya, T. *Chem. Commun.* **2005**, 924.
(9) Benitez, J. J.; Alvero, R.; Capitan, M. J.; Carrizosa, I.; Odriozola, J. A. *Appl. Catal.* **1991**, *71*, 219.
(10) Benitez, J. J.; Alvero, R.; Carrizosa, I.; Odriozola, J. A. *Catal. Today* **1991**, *9*, 53.
(11) Kusama, H.; Okabe, K.; Sayama, K.; Arakawa, H. *Catal. Today* **1996**, *28*, 261.
(12) Fisher, I. A.; Bell, A. T. *J. Catal.* **1996**, *162*, 54.
(13) Kusama, H.; Bando, K. K.; Okabe, K.; Arakawa, H. *Appl. Catal., A* **2001**, *205*, 285.
(14) Marwood, M.; Doepper, R.; Renken, A. *Appl. Catal., A* **1997**, *151*, 223.
(15) Huang, M.; Kaliaguine, S.; Suppiah, S. *Appl. Surf. Sci.* **1995**, *90*, 393.
(16) Erdöhelyi, A.; Pásztor, M.; Solymosi, F. *J. Catal.* **1986**, *98*, 166.
(17) Solymosi, F.; Erdöhelyi, A.; Lancz, M. *J. Catal.* **1985**, *95*, 567.
(18) Ferri, D.; Bürgi, T.; Baiker, A. *Phys. Chem. Chem. Phys.* **2002**, *4*, 2667.
(19) Dardas, Z.; Süer, M. G.; Ma, Y. H.; Moser, W. R. *J. Catal.* **1996**, *159*, 204.
(20) Schneider, M. S.; Grunwaldt, J. D.; Bürgi, T.; Baiker, A. *Rev. Sci. Instrum.* **2003**, *74*, 4121.
(21) Caravati, M.; Grunwaldt, J. D.; Baiker, A. *Phys. Chem. Chem. Phys.* **2005**, *7*, 278.
(22) He, R.; Dava, R. R.; Dumesic, J. A. *J. Phys. Chem. B* **2005**, *109*, 2810.
(23) Fujita, S. I.; Takezawa, N. *Chem. Eng. J.* **1997**, *68*, 63.
(24) Fisher, I. A.; Woo, H. C.; Bell, A. T. *Catal. Lett.* **1997**, *44*, 11.
(25) Ferri, D.; Bürgi, T.; Baiker, A. *J. Phys. Chem. B* **2001**, *105*, 3187.
(26) Grunwaldt, J. D.; Göbel, U.; Baiker, A. *Fresenius' J. Anal. Chem.* **1997**, *358*, 96.
(27) Bürgi, T.; Baiker, A. *J. Phys. Chem. B* **2002**, *106*, 10649.
(28) Ferri, D.; Bürgi, T.; Baiker, A. *Helv. Chim. Acta* **2002**, *85*, 3639.
(29) Grunwaldt, J. D.; Caravati, M.; Ramin, M.; Baiker, A. *Catal. Lett.* **2003**, *90*, 221.
(30) Ferri, D.; Bürgi, T.; Baiker, A. *J. Catal.* **2002**, *210*, 160.
(31) Briggs, D.; Seah, M. P. Practical Surface Analysis. In *Practical Surface Analysis*; Wiley: New York, 1990; Vol. 1.
(32) Jones, M. G.; Nevell, T. G.; Ewen, R. J.; Honeybourne, C. L. **1991**, *70*, 277.
(33) Kim, K. S.; Winograd, N. *J. Catal.* **1974**, *35*, 66.
(34) Aika, K.; Ohya, A.; Ozaki, A.; Inoue, Y.; Yasumori, I. *J. Catal.* **1985**, *92*, 305.
(35) Kawai, M.; Uda, M.; Ichikawa, M. *J. Phys. Chem.* **1985**, *89*, 1654.
(36) Vannice, M. A.; Wang, S. Y. *J. Phys. Chem.* **1981**, *85*, 2543.
(37) Mizushima, T.; Tohji, K.; Udagawa, Y.; Ueno, A. *J. Am. Chem. Soc.* **1990**, *112*, 7887.
(38) Schneider, M. S.; Grunwaldt, J. D.; Baiker, A. *Langmuir* **2004**, *20*, 2890.
(39) Tsang, C. Y.; Streett, W. B. *Chem. Eng. Sci.* **1981**, *36*, 993.
(40) Ke, J.; King, P. J.; George, M. W.; Poliakoff, M. *Anal. Chem.* **2005**, *77*, 85.
(41) Wambach, J.; Baiker, A.; Wokaun, A. *Phys. Chem. Chem. Phys.* **1999**, *1*, 5071.
(42) Shao, C. P.; Chen, M. *J. Mol. Catal. A: Chem.* **2001**, *170*, 245.
(43) Avery, N. R. *Appl. Surf. Sci.* **1982**, *11−2*, 774.
(44) Columbia, M. R.; Crabtree, A. M.; Thiel, P. A. *J. Am. Chem. Soc.* **1992**, *114*, 1231.
(45) Ohtani, T.; Kubota, J.; Wada, A.; Kondo, J. N.; Domen, K.; Hirose, C. *Surf. Sci.* **1996**, *368*, 270.
(46) Sexton, B. A. *Surf. Sci.* **1981**, *102*, 271.
(47) Wang, J. H.; Masel, R. I. *Surf. Sci.* **1991**, *243*, 199.
(48) Singh, U. K.; Vannice, M. A. *J. Catal.* **2000**, *191*, 165.
(49) Singh, U. K.; Vannice, M. A. *J. Catal.* **2001**, *199*, 73.
(50) Burgener, M.; Wirz, R.; Mallat, T.; Baiker, A. *J. Catal.* **2004**, *228*, 152.
(51) Arunajatesan, V.; Subramaniam, B.; Hutchenson, K. W.; Herkes, F. E. Catalysis of Organic Reactions. In *Catalysis of Organic Reactions*; Morrel, D. G., Ed.; Marcel Dekker: New York, 2002; Vol. 89, p 461.

(52) Ma, Z.; Kubota, J.; Zaera, F. *J. Catal.* **2003**, *219*, 404.
(53) Ferri, D.; Bürgi, T.; Baiker, A. *J. Phys. Chem. B* **2004**, *108*, 14384.
(54) Hoshi, N.; Hori, Y. *Electrochim. Acta* **2000**, *45*, 4263.
(55) Xu, J. Z.; Yates, J. T. *Surf. Sci.* **1995**, *327*, 193.
(56) Bos, A. N. R.; Westerterp, K. R. *Chem. Eng. Process.* **1993**, *32*, 1.
(57) McLeod, A. S.; Blackwell, R. *Chem. Eng. Sci.* **2004**, *59*, 4715.